ARTICLE
Journal of Cellular Biochemistry 111:1149–1159 (2010)

Journal of Cellular Biochemistry

Demethyl Fruticulin A (SCO-1) Causes Apoptosis by Inducing Reactive Oxygen Species in Mitochondria

Massimiliano Monticone,[1†] Angela Bisio,[2†] Antonio Daga,[3] Paolo Giannoni,[1] Walter Giaretti,[3] Massimo Maffei,[3] Ulrich Pfeffer,[3] Francesco Romeo,[3] Rodolfo Quarto,[1,4] Giovanni Romussi,[2] Giorgio Corte,[3,5] and Patrizio Castagnola[3*]

[1] *Centro Biotecnologie Avanzate, Genova, Italy*
[2] *Dip. Chimica e Tecnologie Farmaceutiche ed Alimentare, Università di Genova, Genova, Italy*
[3] *Istituto Nazionale per la Ricerca sul Cancro, Genova, Italy*
[4] *Dip. Medicina Sperimentale, Università di Genova, Genova, Italy*
[5] *Dip. Oncologia Biologia e Genetica, Università di Genova, Genova, Italy*

ABSTRACT

Demethyl fruticulin A (SCO-1) is a compound found in *Salvia corrugata* leaves. SCO-1 was reported to induce anoikis in cell lines via the membrane scavenging receptor CD36. However, experiments performed with cells lacking CD36 showed that SCO-1 was able to induce apoptosis also via alternative pathways. To gain some insight into the biological processes elicited by this compound, we undertook an unbiased genomic approach. Upon exposure of glioblastoma tumor initiating cells (GBM TICs) to SCO-1 for 24 h, we observed a deregulation of the genes belonging to the glutathione metabolism pathway and of those belonging to the biological processes related to the response to stress and to chemical stimulus. On this basis, we hypothesized that the SCO-1 killing effect could result from the induction of reactive oxygen species (ROS) in the mitochondria. This hypothesis was confirmed by flow cytometry using MitoSOX, a mitochondria-selective fluorescent reporter of ROS, and by the ability of *N*-acetyl cysteine (NAC) to inhibit apoptosis when co-administered with SOC-1 to the GBM TICs. We further show that NAC also protects other cell types such as HeLa, MG-63, and COS-7 from apoptosis. We therefore propose that ROS production is the major molecular mechanism responsible for the pro-apoptotic effect induced by SCO-1. Consequently, SCO-1 may have a potential therapeutic value, which deserves further investigation in animal models. J. Cell. Biochem. 111: 1149–1159, 2010.

KEY WORDS: GLIOBLASTOMA TUMOR INITIATING CELLS; APOPTOSIS; MITOCHONDRIA; ROS; TERPENOID

Plant extracts are a valuable source of phytochemicals that have diverse uses in medicine. Several of them have cytotoxic activity by inducing apoptosis in many cell types, including cancer cells [Sarkar and Li, 2004; Seeram et al., 2005; Nair et al., 2007; Abdel-Massih et al., 2009; Arlorio et al., 2009; Chung et al., 2009; Kang et al., 2009; Kaur et al., 2009; Park et al., 2009; Ho et al., 2009a,b]. Others display the ability to sensitize cells to the pro-apoptotic activity of other drugs [Jazirehi and Bonavida, 2004; Sarkar and Li, 2004; Alisi and Balsano, 2007]. By this way, also cells that acquired resistance to conventional chemotherapeutic agents can be killed [Jazirehi and Bonavida, 2004; Sarkar and Li, 2004]. Much effort in the field of oncological therapy is therefore dedicated to the discovery of novel phytochemicals able to kill cancer cells either alone or in combination with synthetic drugs.

The epidermal appendages of terrestrial plants contribute to the defense against biotic and abiotic stress [Amme et al., 2005; Slocombe et al., 2008]. The trichomes, that is, the glandular structures of Salvia leaves, secrete an exudate enriched with a

[†]These authors contributed equally to this paper.

Additional Supporting Information may be found in the online version of this article.

Grant sponsor: Regione Liguria (Accordo collaborazione scientifica tra Liguria e Piemonte, per l'anno 2008); Grant sponsor: Compagnia di San Paolo.

Massimiliano Monticone's present address is Istituto Nazionale per la Ricerca sul Cancro, Largo R. Benzi, 10, 16132 Genova, Italy

*Correspondence to: Patrizio Castagnola, Istituto Nazionale per la Ricerca sul Cancro, Largo R. Benzi, 10, 16132 Genova, Italy. E-mail: patrizio.castagnola@istge.it

Received 9 March 2010; Accepted 28 July 2010 • DOI 10.1002/jcb.22801 • © 2010 Wiley-Liss, Inc.
Published online 3 August 2010 in Wiley Online Library (wileyonlinelibrary.com).

mixture of molecules that have antimicrobial and pro-apoptotic activities. The present study focuses on one of these compounds: the demethyl fruticulin A, an ixecetane diterpenoid quinone, also known as *Salvia Corrugata-1* (SCO-1), [Rodriguez-Hahn et al., 1986; Bisio et al., 2008].

In previous studies, we showed that purified SCO-1 had bactericidal and bacteriostatic activities against Gram-positive pathogens [Bisio et al., 2008] and that it induced anoikis, a special form of apoptosis, in mammalian cells [Giannoni et al., 2010].

This anoikis induction was time- and dose-dependent in epithelial HeLa [Giannoni et al., 2010] and MG-63 cell lines and, along with the uptake of the drug from the medium, partially depended on the level of expression of the scavenger membrane receptor CD36. However, SCO-1 also killed COS-1 cells where CD36 is not expressed; this observation led to the hypothesis that SCO-1 could enter the cells and induce apoptosis through CD36-independent pathways [Giannoni et al., 2010].

In the present study, we adopted a quite different cellular model; we used glioblastoma tumor initiating cells (GBM TICs) obtained as long-term cultures in serum-free conditions, as previously reported [Gangemi et al., 2009; Monticone et al., 2009]. The choice of this model was based on the following considerations: (1) GBM, albeit rare, is the fifth cancer-related cause of death; the prognosis of this tumor sadly remains poor even though combined surgical treatments and chemo/radiotherapy regimens have been recently developed; novel strategies and active compounds are therefore highly demanded to better control this disease; (2) it is common opinion that cancer stem cells/TICs are responsible for maintaining and diffusing the tumor in the host; (3) GBM TICs display chemo- and radioresistance properties leading to cancer recurrence; they reflect the properties that cancer stem cells present in the in vivo lesions better than do cancer cell lines maintained and propagated in serum supplemented media [Lee et al., 2006]; they are notoriously resistant to anoikis and can grow in vitro in non-adherent conditions forming neuro-sphere like structures.

To contribute to a better characterization of the molecular pathways and the biological processes underlying the cytotoxic activity of SCO-1, we here decided to pursue an unbiased pharmacogenomic approach by generating the gene expression profile of GBM TICs subjected to the administration of SCO-1 and comparing it with that of control cells exposed to the only vehicle.

Using this approach, we unveiled that the main mechanism responsible for the SCO-1 pro-apoptotic effect is the generation of superoxide in mitochondria. Although SCO-1 does not show a higher activity in TICs as compared with differentiated cells derived from them, this molecule appears to have potential chemotherapeutic properties that should be further investigated in GBM xenotransplant models.

MATERIALS AND METHODS

CELL CULTURES

GBM TICs were obtained from tumor surgical samples provided by the Neurosurgery Department of the San Martino Hospital in Genoa. All patients signed an informed consent before surgery, as required by the Ethical Board.

Cell isolation has been described in details elsewhere [Gangemi et al., 2009]. Growth medium was DMEM-F12/Neurobasal supplemented with 1% (v/v) B27 supplement (Gibco, Ltd., Paisley, Scotland), 2 mM L-glutamine (Gibco, Ltd), recombinant human fibroblast growth factor (FGF-2, 10 ng/ml; Peprotech, London, UK), recombinant human epidermal growth factor (EGF, 20 ng/ml Peprotech). The medium was changed twice a week. As described, TICs grown under these conditions as monolayers in flasks coated with Matrigel (BD Biosciences, San Jose, CA), established long-term cultures, expressed stem cell markers, maintained intact self-renewal capacity and partial multilineage differentiation ability, and gave rise to tumor when injected orthotopically in nude mice [Gangemi et al., 2009]. Cells were split and seeded the day before challenging with chemicals and were monitored by bright field microscopy at each experimental time point.

To rule out possible pro-differentiation effects induced by Matrigel, when indicated, suspension cultures of GBM TICs were performed; neuro-spheres were allowed to form for 4 weeks; thereafter, the cells were seeded and maintained on laminin-coated dishes for 2 weeks, and finally reseeded on laminin 24 h before treatment.

Human osteosarcoma cells (MG63 cells) and transformed human epithelial cells derived from cervical carcinoma (HeLa cells) were obtained from Cell Bank and Cell Factory (Istituto Nazionale per la Ricerca sul Cancro, Genova, Italy). Cells were maintained at 37°C in a humidified atmosphere at 5% CO_2. All MG-63 and HeLa cultures were performed in monolayer using specific media supplemented with 10% fetal bovine serum (FBS; GIBCO—Invitrogen, Milan, Italy). F12-medium (Biochrom AG, Berlin, Germany) and Dulbecco's modified Eagle's Medium (DMEM, high glucose, EuroClone S.p.A., Milan, Italy) were used for MG-63 and HeLa cells, respectively. Medium was changed three times a week.

CHEMICALS

The SCO-1 was obtained lyophilized, with purity ≥99% by HPLC, as previously reported [Bisio et al., 2008; Giannoni et al., 2010], dissolved at 50 mg/ml concentration in dimethyl sulphoxide (DMSO), aliquoted and stored in the dark at −20°C. Equal amounts of DMSO alone were added to all control cultures.

N-acetyl-L-cysteine (NAC) was obtained from Sigma–Aldrich (Schnelldorf, Germany) with purity ≥99% by TLC, dissolved in H_2O at 2 M concentration, aliquoted and stored in the dark at −20°C. Cells were treated with 2 mM NAC, as previously reported for glioma cells [Choi et al., 2004]. Sodium pyruvate was obtained from Sigma–Aldrich with purity ≥99%, dissolved in H_2O at 0.22 mg/ml, aliquoted and stored in the dark at −20°C. When indicated, the culture medium, which already contained 0.36 mM sodium pyruvate, was further supplemented in order to obtain a final concentration of 0.46 mM.

GROWTH KINETICS

Growth was evaluated at different time intervals using the Alamar blue reagent (Invitrogen) according to the manufacturer's instruction. Briefly, before each determination, the medium was discarded and replaced with fresh one containing the reagent. After 3 h of incubation 37°C in a humidified atmosphere at 5% CO_2, the

supernatant was collected and its absorbance at 570 nm was spectrophotometrically assessed. Results were normalized to the values obtained from control cells at the onset of the experiment. Cell growth for the different experimental conditions was then expressed as normalized absorbance values.

The IC50s for GBM TICs derived from Patient 1 (PT1), GBM TICs derived from Patient 2 (PT2), HeLa, MG-63 and COS-7, calculated as the concentration able to reduce at 50% cell viability after 48 h, were: 9.3, 16.0, 25, 5, and 160 μg/ml, respectively.

FLUOROCHROMES AND FLOW CYTOMETRIC ANALYSIS

Cells harvested with their media to ensure collection of floating cells along with adherent cells were centrifuged at 980*g* for 5 min.

To measure the DNA content in cell nuclei, each sample was stained with 4,6-diamidino-2-phenylindole-2-hydrocloride (DAPI), as described by Otto [1994]. Briefly, one million cells were incubated in 2 ml of detergent solution (0.1 M citric acid, 0.5% Tween-20 in water) for 20 min at RT. Nuclei were passed over a nylon sieve with a pore size of 50 μm (CellTrics yellow filters; Partec GmbH, Münster, Germany), pelletted, resuspended in 200 μl of detergent solution and incubated for 10 min at RT with gentle shaking. Finally, six volumes of staining solution (0.4 M Na_2HPO_4, 5 μM DAPI in water) were added. Each sample was then analyzed, after 15 min of incubation using a CyflowML multiparameter flow cytometer (Partec). Excitation of DAPI was provided by an UV mercury lamp (HBO-100 long life, 100W) and the emitted fluorescence was collected by the Gratz setting (488 blue solid laser shut down; 435 nm long pass filter).

To determine the extent of apoptosis and necrosis, cells were labeled with sytox blue, Resorufin, and allophycocyanin (APC)-conjugated annexin V (Invitrogen). To determine superoxide anion generation in mitochondria, cells were labeled with MitoSOX Red (Invitrogen) according to the manufacturer's instruction. Samples were subjected to flow cytometric analysis using a CyAn ADP analyzer equipped with 405, 488, and 635 nm lasers and 450/60, 575/25, and 665/20 nm band pass filters to detect the above fluorochromes (Dako, Glostrup, Denmark).

RNA EXTRACTION AND QUALITY ANALYSIS

Total RNA was isolated using the miRNeasy® mini kit (Qiagen, Hilden, Germany) including DNase treatment. RNA concentration and purity were determined by absorbance at both 260 and 280 nm; 2 μg total RNA were run on a 1% denaturing gel and 100 ng were loaded on the 2100 Bioanalyzer (Agilent, Palo Alto, CA) to verify RNA integrity.

AMPLIFICATION OF RNA AND ARRAY HYBRIDIZATION

According to the recommendations of the manufacturer, 100 ng of total RNA were used in the first-round synthesis of double-stranded cDNA. The RNA was reverse transcribed using a Whole Transcript cDNA synthesis and amplification kit (Affymetrix UK, Ltd., High Wycombe, UK). The resulting biotin-labeled cRNA was purified using an IVT clean-up kit (Affymetrix) and quantified using a UV spectrophotometer (A260/280; Beckman, Palo Alto, CA). An aliquot (15 μg) of cRNA was fragmented by heat and ion-mediated hydrolysis at 94°C for 35 min. Fragmented cRNA, run on the Bioanalyzer (Agilent Technologies, Santa Clara, CA) to verify the correct electropherogram, was hybridized in a hybridization oven (16 h, 45°C) to a Human Gene 1.0 ST array (Affymetrix) representing whole-transcript coverage. Each one of the 28,869 genes is represented on the array by approximately 26 probes spread across the full length of the gene, providing a more complete and more accurate picture of gene expression than the 3′-based expression array design. The washing and staining procedures of the arrays with phycoerythrin-conjugated streptavidin (Invitrogen) was completed in the Fluidics Station 450 (Affymetrix). The arrays were subsequently scanned using a confocal laser GeneChip Scanner 3000 7G and the GeneChip Command Console (Affymetrix).

GENECHIP MICROARRAY ANALYSIS AND DATA NORMALIZATION

Affymetrix raw data files [cell intensity (CEL) files] were used as input files in expression console environment (Affymetrix). Briefly, CEL files were processed using the Robust Multi-Array Analysis (RMA) procedure [Irizarry et al., 2003], an algorithm that is publicly available at http://www.bioconductor.org. The RMA method was used for pre-processing to obtain a single expression value for each probe set and normalization by sketch quantile normalization. Quality assessments were also performed in the expression console environment. This procedure, based on various metrics, allowed us to identify a chip as an outlier (see for details Quality assessment of exon and gene arrays http://www.affymetrix.com/support/technical/whitepapers/exon_gene_arrays_qa_whitepaper.pdf). We identified the transcripts whose expression was regulated more than threefold using MS Excel software (Microsoft Corp., Redmond, WA). Hierarchical Clustering (HCL), after mean scaling and log 2 transformation, were performed with the software tool from The Institute for Genomic Research (TIGR) MeV (multiple experimental viewer) (http://www.tigr.org/software/tm4/mev.html) [Saeed et al., 2003].

All the microarray information has been submitted to the National Center for Biotechnology Information Gene Expression Omnibus web site (http://www.ncbi.nlm.nih.gov/geo/query/acc.cgi?acc=GSE19846).

PATHWAYS IDENTIFICATION BY EXPRESSION ANALYSIS SYSTEMIC EXPLORE (EASE)

Gene lists from Affymetrix results were examined using the EASE program, accessible via http://david.abcc.ncifcrf.gov/. EASE is a customized stand-alone software application with statistical functions for discovering biological themes within gene lists [Hosack et al., 2003]. This software assigns genes of interest into functional categories based on the Gene Ontology database (GO, http://www.geneontology.org/index.shtml) and uses the Fisher's exact test statistics to determine the probability of observing the number of genes within a list of interest versus the number of genes in each category on the array. A more detailed analysis of the genes' association with physiological pathways was performed using the Kyoto Encyclopedia of Genes and Genomes (KEGG, http://www.genome.jp/kegg/pathway.html). Each identified process was confirmed through PubMed/Medline (http://www.ncbi.nlm.nih.gov/sites/entrez?db=pubmed).

RT-PCR ANALYSIS

Starting from about 1 μg of total RNA, cDNA was synthesized by using an Oligo(dT)20, random hexamers mix, and a Superscript III first-strand synthesis system supermix for RT-PCR (Invitrogen). cDNAs were diluted 5–20 times and then subjected to PCR analysis.

Relative quantification was performed by real-time quantitative RT-PCR (qPCR). Briefly, qPCR was performed and analyzed using real-time PCR (Real Plex^2; Eppendorf S.r.l., Milan, Italy). Primers were designed across a common exon–exon splice junction by using the tool available at https://www.roche-applied-science.com/sis/rtpcr/upl/index.jsp?id=UP030000 (Roche Applied Science, Monza, Italy) to avoid possible signal production from potential contaminating genomic DNA (see Supplementary Material 1). Reactions were carried out in triplicates and amplicons were measured by SYBR Green fluorescence (5 Prime, Hamburg, Germany) according to manufacturer's recommendations. Specificity of the products was verified by thermal dissociation analysis.

The gene coding for the ribosomal protein L14 (*RPL14*) was used as the endogenous control for normalization because, in the microarray data, it showed in all conditions the steadiest expression in our experimental setting as compared with other housekeeping genes.

RESULTS

SCO-1 KILLS GBM TICS IN CULTURE IN A DOSE-DEPENDENT MANNER

To determine whether SCO-1 has any effect on GBM TICs in vitro, cells obtained from PT1 were cultured with medium alone or supplemented with different amounts of DMSO (vehicle-control treatment) and SCO-1. After 48 h, the cell viability was determined by the Alamar blue test. PT1 GBM TICs treated with SCO-1 displayed a dose-dependent reduction of cell viability as compared with control cells (Fig. 1). The concentration yielding about 50% killing activity (IC50) in the GBM TICs after 48 h of continuous exposure was 9.3 μg/ml. Similar dose–response curve experiments were performed in order to determine the IC50 specific for each cell type used in this study (see Materials and Methods section). Unless otherwise indicated, IC50 were used in the subsequent experiments. Cultures treated with increasing concentration of SCO-1 displayed a parallel reduction of cells adherent to the substrate and an increase of round cells loosely attached to the substrate or floating in the medium (data not shown).

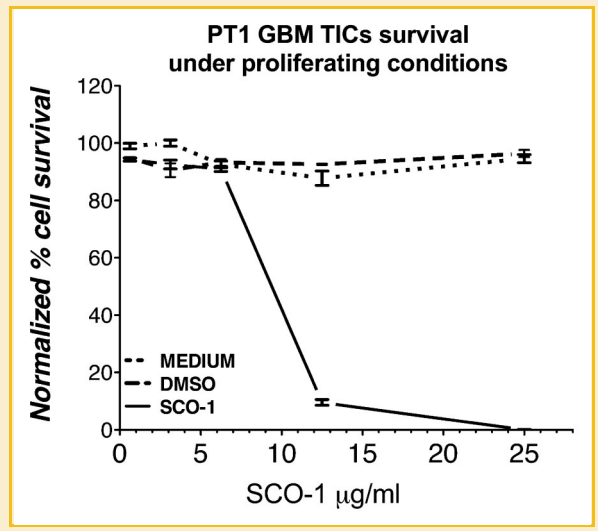

Fig. 1. SCO-1 kills GBM TICs in culture. Survival curves of GBM TICs cells derived from PT1 based on the results of Alamar blue assays after 48 h of exposure to SCO-1 in growth medium or to medium/DMSO matched controls. Average values from at least three independent experiments are shown. Standard deviations are indicated as vertical bars.

SCO-1 AFFECTS THE EXPRESSION OF GENES HAVING A ROLE IN THE UP-REGULATION OF GLUTATHIONE METABOLISM PATHWAY, RESPONSE TO STRESS AND CHEMICAL STIMULUS, AND CELL CYCLE ARREST

To investigate the molecular basis underlying the SCO-1-induced apoptosis in GBM TICs, we determined the gene expression profile of these cells after 24 and 48 h of exposure to SCO-1 and DMSO using GeneChip microarrays. To gain a mechanistic understanding of the processes affected by SCO-1, the EASE program and the EASE score [Hosack et al., 2003] were used to identify GO functional categories that were significantly over-represented. After filtering the results to avoid redundant and/or generic categories, statistically significant GO terms associated with SCO-1-regulated genes were found (Table I).

The results clearly showed that the genes whose expression changed by a factor 3 after treatment with SCO-1 in the PT1 cells were associated with glutathione metabolism pathway, response to stress and chemical stimulus at 24 h (Table I), and to cell cycle, cell proliferation, response to stress, and p53-signaling pathway at the 48 h time-point (Table I). In particular, after 24 h, SCO-1 induced the up-regulation of the genes *GCLM*, *GCLC*, *MGST1*, *GSTM3*, and *GPX3* whereas after 48 h SCO-1 down-regulated several genes associated with cell cycle, cell proliferation, and up-regulated several genes having a role as inhibitors of these processes (Table I). Differential expression by the GBM TICs treated with SCO-1 and DMSO of the genes included in Table I was visualized by a heat map visualization obtained by HCL which generates a tree (dendrogram) to group similar objects together (see Supplementary Material 2).

Changes in mRNA expression levels were confirmed in an experimental replica by real-time PCR analysis of arbitrarily selected genes (*DDIT3*, *PPP1R15A*, *GCLC*, *GCLM*, *PCNA*, and *CCNA2*), which resulted deregulated from the gene array experiments (Fig. 2). A complete list of genes significantly regulated in the comparison between the SCO-1 versus DMSO-treated GBM TICs is provided (see Supplementary Material 3).

SCO-1 INDUCES APOPTOSIS IN GBM TICS, WHICH IS ABOLISHED BY CONCOMITANT ADMINISTRATION OF *N*-ACETYL-L-CYSTEINE (NAC).

To investigate the killing mechanism underlying the activity of SCO-1 in GBM TICs, we took advantage of a multi-color labeling system able to detect apoptosis and necrosis at the same time. This system employs the use of APC-conjugated annexin V, C_{12}-resazurine and sytox blue to discriminate metabolically active cells, early apoptotic,

TABLE I. Gene Ontology and KEGG Pathway Analyses of the Comparison Between the SCO1-Treated (9.3 μg/ml) and the Control (DMSO) GBM TICs From PT1

System gene category term	Count	%	*P*-value	Most regulated genes
SCO-1 vs. DMSO-24 h exposure				
GO biological process				
Response to stress	42	16.73	3.62E-10	***HMOX1***, ***HSPB8***, ***CYP4F11***, ***GCLM***, ***HSPA1B***, ***DNAJB4***, ***DDIT3***, ***SRXN1***, *TYMS*, *SCG2*, *ID3*, *CCND1*, *HIG2*, *PTX3*, *TGFB2*, *TXNIP*
Response to chemical stimulus	29	11.55	5.16E-09	***HMOX1***, ***HSPB8***, ***GCLM***, ***HSPA1B***, ***DNAJB4***, ***DDIT3***, ***SRXN1***, ***ME1***, *CCL2*, *SCN11A*, *SCG2*, *STC1*, *CCND1*, *KCNIP1*, *TGFB2*, *TXNIP*
KEGG_pathway				
Glutathione metabolism	5	1.99	6.25E-03	***GCLM***, ***GCLC***, ***MGST1***, ***GSTM3***, ***GPX3***
SCO-1 vs. DMSO-48 h exposure				
GO biological process				
Cell cycle	71	16.80	1.6E-21	***DDIT3***, ***PPP1R15A***, ***EREG***, ***CDKN1A***, ***IL8***, ***SESN2***, ***CYLD***, ***CCPG1***, *CDC7*, *CDCA3*, *TXNIP*, *TGFB2*, *CDC2*, *SPC25*, *FBXO5*, *NCAPH*
Cell proliferation	53	12.60	8.9E-13	***HMOX1***, ***GPNMB***, ***EREG***, ***CDKN1A***, ***MXD1***, ***IL8***, ***MAFG***, ***TXNRD1***, *TGFB2*, *GPC4*, *SCG2*, *ADRA1A*, *CDCA7*, *SERPINF1*, *KIT*, *FABP7*
Response to stress	52	12.30	1.20E-07	***HMOX1***, ***HSPB8***, ***CYP4F11***, ***GCLM***, ***DDIT3***, ***PPP1R15A***, ***HSPA1B***, ***EREG***, *TYMS*, *CCNA2*, *TXNIP*, *TGFB2*, *POLE2*, *TOP2A*, *SCG2*, *CDC2*
KEGG_pathway				
Cell cycle	18	4.27	5.64E-09	***CDKN1A***, ***GADD45B***, *CCNB1*, *MAD2L1*, *BUB1*, *MCM5*, *MCM7*, *BUB1B*, *CDK2*, *PCNA*, *MCM6*, *SKP2*, *CCNA2*, *CDC7*, *TGFB2*, *CDC2*
p53-signaling pathway	9	2.13	4.28E-04	***CDKN1A***, ***SERPINE1***, ***SESN2***, ***TNFRSF10B***, ***GADD45B***, *CHEK1*, *CCNB1*, *CDK2*, *CDC2*

Non-redundant functional categories, number of genes contained within each category and percentages ranked by the degree of over-representation in the category as determined by EASE (*P*-value) are shown. Redundant categories sharing more than 50% gene members were removed to yield a single representative category. Up to 16 of the most regulated gene members, ordered from the most up-regulated gene (bold font) to the most down-regulated one (regular font) are shown in the last column. Only categories associated with a *P*-value <0.02 and with a *P*-value <5E-7 are shown for KEGG pathway and for the GO biological processes, respectively.

late apoptotic, and necrotic cells. The non-fluorescent C_{12}-resazurine is reduced to orange-fluorescent resorufin by live cells, the far-red fluorescent APC-annexin V binds to exposed phosphatidylserine on the membrane of apoptotic cells and sytox blue, being unable to permeate living cells, is able to bind to the DNA of cells with compromised membranes such as late apoptotic and necrotic cells. These cell subpopulations can be discriminated by flow cytometry. After 24 h of treatment with SCO-1, PT1 GBM TICs showed a reduction in the resorufin$^+$/sytox$^-$ cell subpopulations (metabolic active cells with intact membrane) and an increase in both the annexin V$^+$/sytox$^+$ and in the annexin V$^+$/resorufin$^-$ cell subpopulations (late apoptotic) as compared with the DMSO treatment (R5, R7 and R13, respectively in Fig. 3).

To prove that ROS generation and GSH depletion are the main molecular mechanisms induced by SCO-1, which lead GBM TICs to apoptosis, we treated these cells with an antioxidant compound. We argued that if this hypothesis were true, the antioxidant should rescue GBM TICs from the killing effect of SCO-1. NAC was used since it contains a thiol group with a direct antioxidant effect and is a precursor of cysteine, which concentration is the rate-limiting step of glutathione synthesis (L-gamma-glutamyl-L-cysteinylglycine).

To better assess the effect of NAC on the apoptotic induction by SCO-1, we performed a multiplex (sytox blue/resazurine/annexin V APC) flow cytometry analysis. NAC and SCO-1 treated GBM TICs for 24 h displayed a strong reduction of both the sytox$^+$/resorufin$^-$ subpopulation (cells metabolically inactive with compromised membrane, R2 in Fig. 3), and the annexin V$^+$/resorufin$^-$ subpopulation (late apoptotic cells, R13 in Fig. 3) as compared with cells treated with SCO-1 alone.

In particular, we treated GBM TICs with both SCO-1 and NAC and subjected the cells to Alamar blue cell viability test, bright field microscopy analysis, and flow cytometry analysis for apoptosis and ROS production. Cultures treated for 48 h with NAC and SCO-1 exhibited a cell viability higher than that shown by cells treated with SCO-1 alone and similar to control cells (Fig. 4). Microscopy analysis revealed that cells treated for 48 h with NAC and SCO-1 exhibited a less pronounced birefringent rounded phenotype, a reduced number of floating cells and an increased number of adherent and spread cells as compared with GBM TICs treated with SCO-1 alone (data not shown).

To establish whether ROS generation by SCO-1 is a general mechanism underlying death of eukaryotic cells in culture, we subjected also the epithelial HeLa and the mesenchymal MG-63 cell lines to the combined treatment with SCO-1 and NAC and evaluated cellular morphology and viability by microscopy and by the Alamar blue reduction assay, respectively. Bright field microscopy analysis of these cells treated with both SCO-1 and NAC showed a reduction of birefringent floating cells as compared with cultures treated with SCO-1 alone (see Supplementary Material 4). The Alamar blue assay indicated that both HeLa and MG-63 cells treated with SCO-1 for 48 h were rescued by NAC from the SCO-1 induced apoptosis (see Supplementary Material 4). Similar results were obtained with the simian COS-7 cells that lack CD36 (see Supplementary Material 4).

In addition, to verify whether a known reducing agent with a chemical structure unrelated to NAC was also able to reduce the SCO-1 pro-apoptotic effect on GBM TICs, these cells (derived from PT2) were treated with SCO-1 together with sodium pyruvate and cell survival was measured after 48 h. We found that, although to a lesser extent than NAC, the cells treated with sodium pyruvate showed a statistically significant higher survival ($P = 0.0034$) with respect to those treated only with SCO-1 (see Supplementary Material 5).

No protection effect was observed when NAC or pyruvate where administrated 24 h either before or after SCO-1 (data not shown).

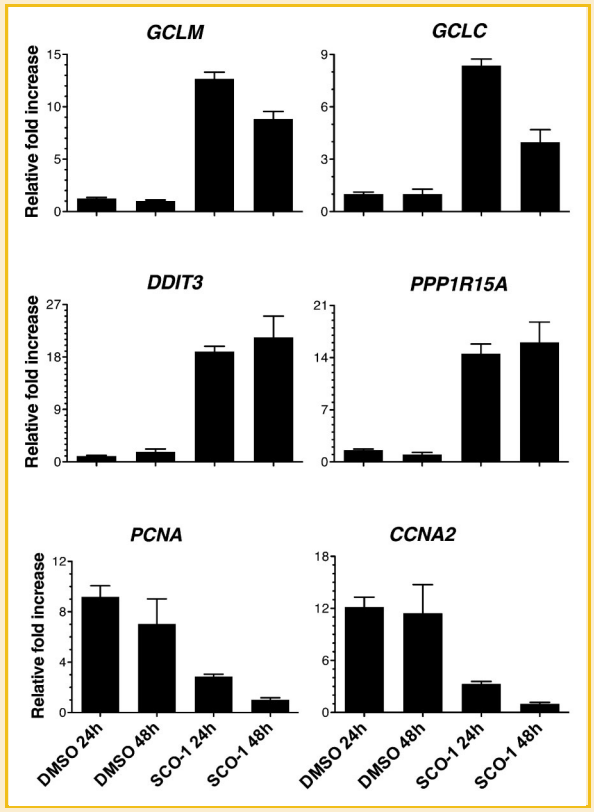

Fig. 2. Real-time RT-PCR validation of microarray data. Real-time RT-PCR analysis performed on GBM TICs derived from PT1 treated with 0.019% DMSO (v/v) or with 9.3 μg/ml (IC50) SCO-1 in growth medium for the indicated time period to validate the microarray data. This was accomplished on randomly selected genes from Table I and shows, in arbitrary units, SCO-1-dependent regulation of gene expression. Expression levels are relative to the expression of the housekeeping ribosomal protein L14 (*RPL14*) gene. Standard deviations are indicated as vertical bars. Gene name symbols used are those approved by the Human Genome Organization Gene Nomenclature Committee (http://www.genenames.org/).

SCO-1 INDUCES GENERATION OF REACTIVE OXYGEN SPECIES (ROS) IN THE MITOCHONDRIA OF GBM TICS

We hypothesized that the up-regulation we observed for several genes belonging to the glutathione metabolism pathway resulted from the generation of ROS in SCO-1 treated cells. We argued that these ROS would cause the depletion of reduced glutathione (GSH) and that, by a feed-back mechanism, this would in turn enhance the expression of genes coding for enzymes involved in the generation of GSH. Based on SCO-1 molecular structure and on the previously demonstrated quinolone-induced generation of ROS, we hypothesized that the mitochondria was the sub-cellular component where ROS were generated by SCO-1. Accordingly, we took advantage of the availability of superoxide indicator selectively targeted to mitochondria named MitoSOX Red, as mitochondria are the major source of ROS within the cell [Cataldi, 2010]. Once oxidized, this reagent becomes fluorescent and allows the identification of ROS production in the mitochondria of living cells since the superoxide anion is the predominant ROS generated in this compartment. We thus challenged PT2 GBM TICs with SCO-1 and DMSO for 48 h, incubated them with MitoSOX Red and then analyzed them by flow cytometry. The comparison of the plots generated by DMSO or SCO-1 treated GBM TICs, revealed that cells in the latter sample displayed a brighter fluorescence emission (Fig. 5) and that ROS generation was consequently higher in mitochondria of SCO-1 treated than in control GBM TICs.

To establish whether NAC was able to inhibit the superoxide generation in mitochondria of cells co-treated with SCO-1, a flow cytometry analysis of PT2 GBM TICs labeled with MitoSOX Red was performed after 48 h of treatment. NAC and SCO-1 treated cultures showed a reduction of the fluorescence emission with respect to the cells treated with SCO-1 alone, indicating a reduction of mitochondrial ROS generation in the concomitant presence of NAC (Fig. 5). Cells treated with NAC only showed a fluorescence emission intermediate between those of control and of SCO-1 treated cells, and very similar to that displayed by cells treated with NAC and SCO-1 (Fig. 5).

SCO-1 INDUCES CELL CYCLE ARREST AND MITOTIC CATASTROPHE IN GBM TICS

On the basis of the results from the EASE analysis, we also hypothesized that GBM TICs would undergo cell cycle arrest and mitotic catastrophe following SCO-1 treatment. To test this hypothesis, we analyzed the nuclear DNA content by DAPI staining of TICs after 48 h of treatment with SCO-1 and DMSO. Since this dye binds to DNA in a stoichiometric ratio and increases its fluorescent emission dramatically with respect to the unbound state, DNA content can be derived from the intensity of the fluorescent signal assessed by flow cytometry. In Figure 6, the DNA content of untreated nuclei in the G0+G1 phase peaked at about 200 units of fluorescent light emission, while G2 + M nuclei had a DNA content corresponding to the double value of 400 units and S phase nuclei had fluorescence values comprised between 200 and 400 units. After 48 h of treatment with SCO-1, PT1 GBM TICs showed an increase of the peak corresponding to G2 + M nuclei as compared with the DMSO-treated PT1 GBM TICs (Fig. 6). In addition, in these SCO-1 treated cells, we observed the appearance of particles corresponding to fragmented (apoptotic) nuclear bodies having lower fluorescent emission, hence lower DNA content, than G0+G1 nuclei (Fig. 6).

CULTURE SUBSTRATE DOES NOT AFFECT SENSITIVITY OF GBM TICS TO SCO-1

Since other researchers reported cell culturing GBM TICs in adherent condition on laminin-coated plastic vessels [Pollard et al., 2009], we performed a SCO-1 treatment of PT2 GBM TICs to assess whether culturing on different substrates may affect cell sensitivity. In particular, cells from a long term established culture of PT2 GBM TICs grown on matrigel were first cultured for 4 weeks in non-adherent culture as neurosphere-like cell clusters; these clusters were then dissociated and the cells were plated on laminin to be further subcultured for 2 weeks. The day before the experiment, cells were re-seeded again on laminin. DMSO, SCO-1, or SCO-1 plus NAC were added to the culture medium and the Alamar test was performed after 48 h. For comparison purposes, a parallel culture of PT2 GBM TICs grown on matrigel at the same cell density (10^5 cells/

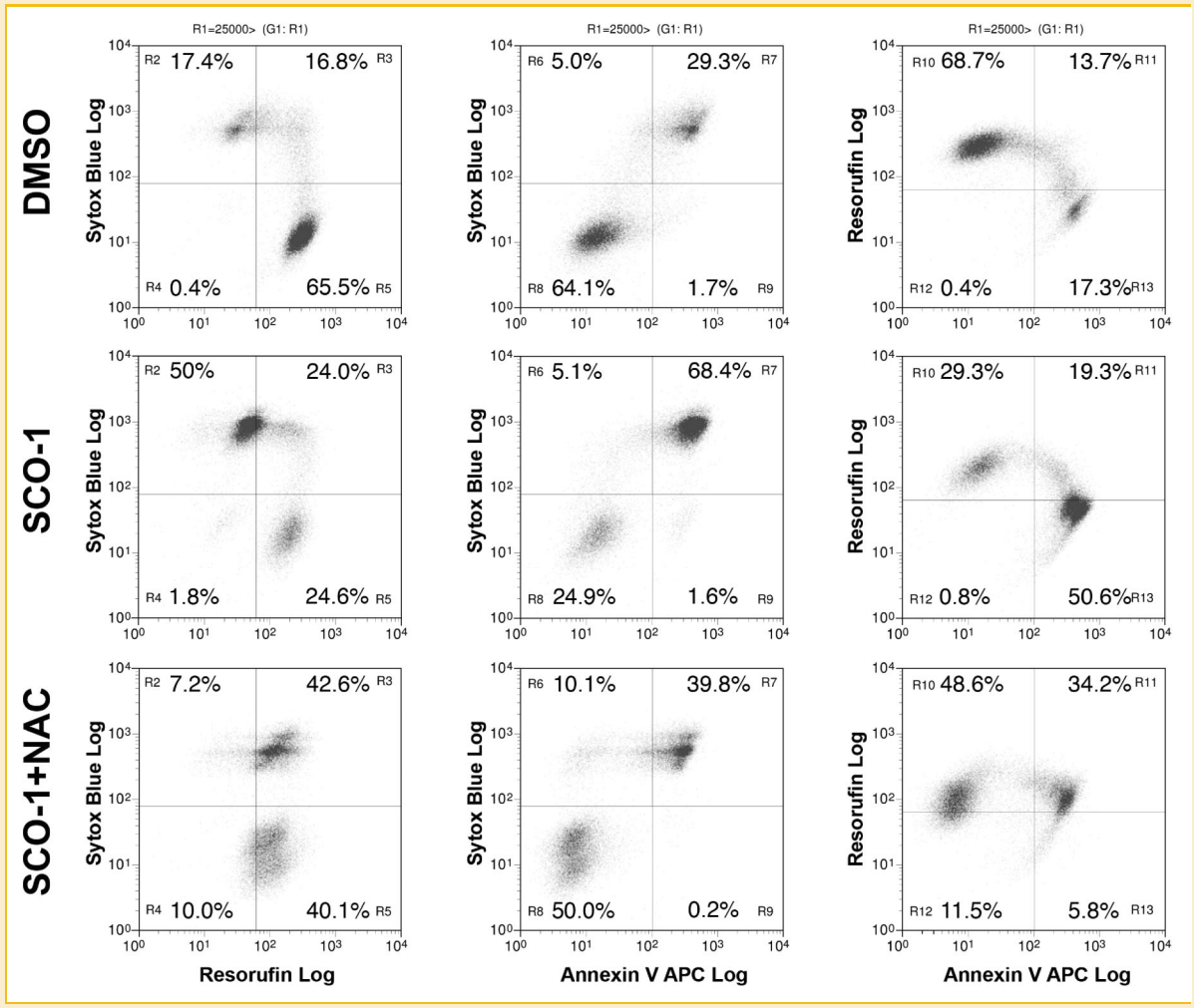

Fig. 3. NAC rescues GBM TICs from the apoptotic effect of SCO-1. Flow cytometric analysis of GBM TICs derived from PT1 after 48 h of exposure to compounds in growth medium. Concentration were: 0.019% (v/v) DMSO (vehicle); 9.3 μg/ml SCO-1 (IC50); 9.3 μg/ml and 2 mM, SCO-1 and NAC, respectively. Cells were labeled with sytox blue, resorufin, and allophycocyanin (APC)-conjugated annexin V.

well of a 24 wells plate) was treated similarly. No major differences were observed in cell viability after SCO-1 treatment and rescue ability of NAC between GBM TICS cultured on either one of the two substrates (Fig. 7). These experiments also showed that when PT2 GBM TICs were treated at SCO-1 concentrations lower than IC50, the cell survival was higher than in control cells (Fig. 7). We hypothesized that SCO-1, at this concentration range, could either inhibit apoptosis or enhance proliferation or perform both tasks. To verify this hypothesis we performed an apoptosis assay and a Ki67 staining (the Ki67 antibody recognizes a nuclear protein encoded by the MKI67 associated and required to maintain cell proliferation) by flow cytometry analysis of PT2 GBM TICs treated with 4.65 μg/ml of SCO-1 or with matching DMSO concentration. We found a reduced percentage of cells double-labeled for annexin V and sytox blue (late apoptotic cells) and a very mild increased expression of Ki67 in cells treated with this concentration of SCO-1 as compared with DMSO-treated cells (data not shown). These results indicate that concentrations of SCO-1 lower than those required to kill 50% of treated cells in 48 h, may indeed induce cell proliferation by a reduced tendency of the cells to undergo apoptosis and, possibly, by a slight increase in proliferation ability.

DISCUSSION

The goal of this study was to establish the main molecular mechanisms responsible for the in vitro pro-apoptotic activity of SCO-1, an ixecetane diterpenoid quinone component of the exudates from Salvia leaves. A previous study showed that this compound induced anoikis, a type apoptosis induced in mammalian cells through a loss of cell adhesion mediated by CD36 [Giannoni et al., 2010]. The same report, however, suggested the existence of alternative, yet undisclosed, apoptotic pathways that could possibly explain the SCO-1 induced death observed in $CD36^{-}$ cells and the incomplete rescue displayed by CD36 blockade with specific antibodies [Giannoni et al., 2010].

To reveal these alternative pathways, we undertook an unbiased pharmacogenomic approach by determining changes in the gene

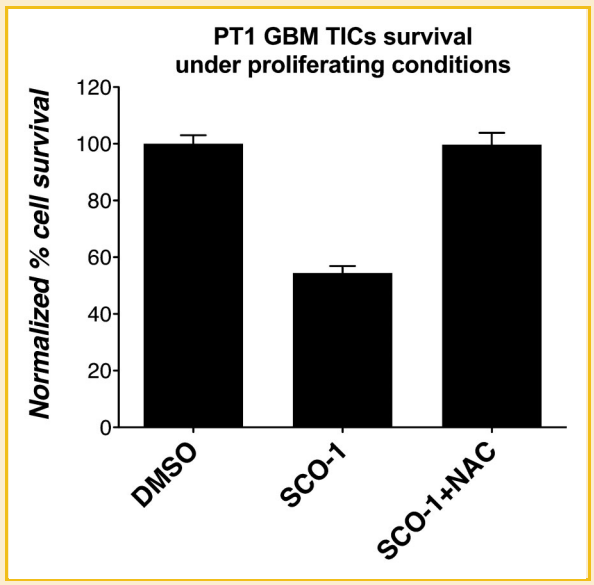

Fig. 4. Survival of GBM TICs treated with SCO-1 is greatly enhanced by NAC. Survival of GBM TICs derived from PT1 after exposure to compounds for 48 h in growth medium. Concentration were: 0.019% (v/v) DMSO (vehicle); 9.3 μg/ml SCO-1 (IC50 for PT1); 9.3 μg/ml and 2 mM, SCO-1 and NAC, respectively. Average values, based on the results of Alamar blue assays, from at least three independent experiments are shown and standard deviations are indicated as vertical bars.

expression profile induced by SCO-1 in GBM TICs. These cells were selected for this study because they are resistant to anoikis, as shown by their ability to grow even in adhesion-independent conditions forming sphere as long as the diffusion rate of nutrients and O_2 is not impaired [Woolard and Fine, 2009].

The results reported here clearly indicate that the genes mostly affected by SCO-1 were first those belonging to the glutathione pathway and later those required to accomplish the different steps of the cell cycle. GBM TICs treated with SCO-1 were also shown to express to a higher extent genes able to actively inhibit these processes, in particular those belonging to the p53-signaling pathway.

More in details, up-regulation of GCLM, GCLC, MGST1, GSTM3, GPX3 in GBM TICs was observed after 24 h of treatment. The enhanced expression of these genes prompted us to establish whether SCO-1 was able to generate ROS within the cell. Using a selective mitochondria superoxide reporter [Robinson et al., 2006], we found that cells challenged with this compound indeed displayed an enhanced production of mitochondrial superoxide. As a further confirmation that we identified the major molecular mechanism of the acute cellular toxicity of SCO-1, both the superoxide generation and the pro-apoptotic activity of SCO-1 were greatly inhibited by the antioxidant NAC and to a lesser extent by sodium pyruvate. Therefore, we concluded that most of the ROS generated by SCO-1 in the mitochondria were released into a water domain since both NAC and sodium pyruvate are hydrophilic molecules [Liu and Schubert, 2009]. Furthermore, we showed that this mechanism is independent from the cell type used since similar results were obtained after the co-administration of NAC and SCO-1 also to HeLa, MG-63, and COS-7 cell lines.

We wish to point out that no protection effect was observed when NAC or pyruvate where administrated 24 h either before or after SCO-1 (data not shown).

Therefore, we cannot rule out that a direct inactivation of SCO-1 is responsible for the inhibition of its cellular effects. However, the evidence that two antioxidants with unrelated chemical structure inhibited the cellular apoptosis induced by SCO-1, suggests that this possibility is unlikely.

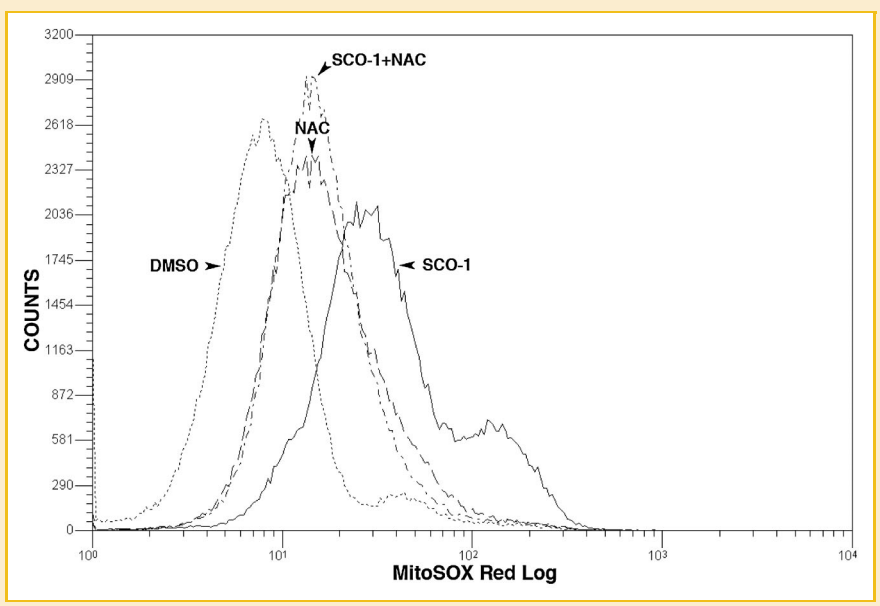

Fig. 5. NAC inhibits SCO-1-induced ROS generation by GBM TICs. Flow cytometric analysis of GBM TICs derived from PT2 after exposure to compounds for 48 h in growth medium. Concentration were: 0.032% (v/v) DMSO (vehicle), dotted line; 16 μg/ml SCO-1 (IC50 for PT2), continuous line; 2 mM NAC, dashed line; 16 μg/ml and 2 mM, SCO-1 and NAC, respectively, dotted and dashed line. Cells were labeled with MitoSOX Red.

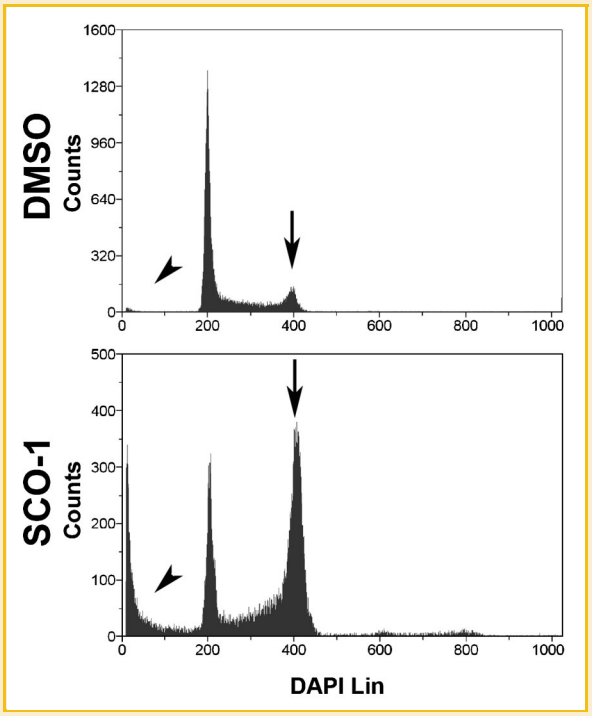

Fig. 6. SCO-1 induces cell cycle arrest in G2+M phase. High resolution flow cytometric analysis of DAPI-stained nuclei of PT1 GBM TICs derived from PT1 after exposure to compounds for 48 h in growth medium. Concentration were: 0.019% (v/v) DMSO (vehicle); 9.3 μg/ml SCO-1 (IC50 for PT1). This analysis reveals the increase of nuclei/fragment having a sub-G1 DNA content (arrow heads) and of nuclei in the G2 and M phase of the cell cycle (arrows) in cells treated with SCO-1 with respect to cells treated with DMSO.

We also observed that NAC alone induced a moderate production of mitochondrial superoxide in GBM TICs. This apparent paradox is not unexpected since it has been reported by others in a different experimental context [Chan et al., 2001].

We suggest that the induction of genes of the glutathione pathway results from a feedback mechanism unleashed by SCO-1 depletion of the GSH pool within the cell. As SCO-1 has a quinone group, this mechanism is in line with the known effects of quinone redox cycling [Koster, 1991; O'Brien, 1991]. In addition, it is possible that the depletion of GSH after exposure to SCO-1 may also indirectly arise from the ROS stress. This may be induced by the generation of superoxide during the quinone redox cycling and cause oxidation of thioles-containing proteins within the cells requiring just GSH to revert to their reduced state. Interestingly, a similar inductive effect on GCLM and GCLC gene expression was observed, that is, after exposure of human HBE1 cells to different oxidative stressors including quinones [Krzywanski et al., 2004]. As some anticancer quinones acquire alkylating properties after intracellular reduction promoted by enzymes of the glutathione pathway, the up-regulation of genes belonging to this pathway is a known and double-sided mechanism [Koster, 1991]. In fact, the induction of the glutathione peroxidase pathway appears to help certain human tumor cells to become partially resistant to anticancer quinones [Akman et al., 1990; Doroshow et al., 1990].

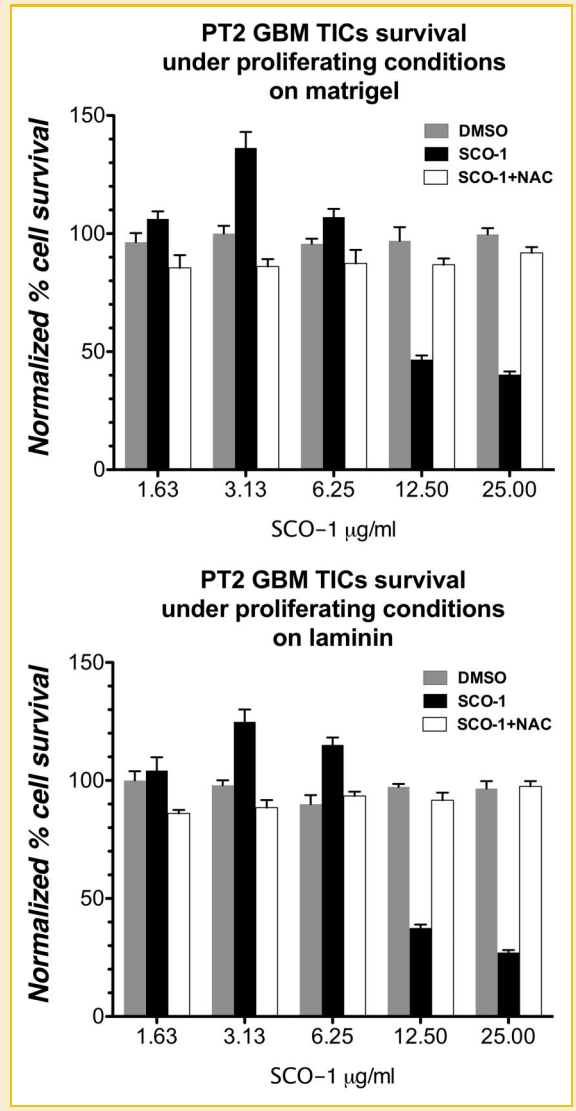

Fig. 7. Survival of GBM TICs treated with SCO-1 is independent from adhesion substrate. Survival of GBM TICs cells derived from PT2 cultured in growth medium based on the results of Alamar blue assays after 48 h of exposure to SCO-1, SCO-1 and NAC or to DMSO matched controls. SCO-1 concentrations were as indicated; NAC concentration was 2 mM. Average values from at least three independent experiments are shown. Standard deviations are indicated as vertical bars.

Here, we also show that GBM TICs challenged with SCO-1 at the IC50, undergo a G2+M cell cycle arrest concomitant to the appearance of sub G0/G1 nuclei, or nuclear fragments, and annexin V binding, which are both indicative of apoptosis. These effects were likely the results of the inhibition of the cell cycle genes and of the induction of some key genes of the p53 pathway (*CDKN1A*, *SERPINE1*, *SESN2*, *TNFRSF10B*, *GADD45B*), as revealed by the gene expression analysis after 48 h of exposure to SCO-1. Results reported by several groups are along this line and similarly show that transfer of p53 or of other proteins belonging to the p53-signaling pathway (including P21/CDK1A), specifically in glioma cells, may induce growth arrest and apoptosis [Fueyo et al., 2001].

We suggest that this deregulation may be due either to the stress-induced activation of p53 by the mitochondrial superoxide generated by SCO-1, or to an activated form of SCO-1 behaving as an alkylating agent, or to both mechanisms. Mitochondrial ROS are indeed known critical intracellular determinants of the p53 stress sensitivity [Karawajew et al., 2005]. On the other hand, when we treated GBM TICs cells with suboptimal SCO-1 concentration, we found a higher survival with respect to control cells. This observation is likely due to a reduced apoptosis tendency, possibly combined with a slightly higher proliferation ability (data not shown). These results are in line with published literature showing that a moderate exposure to ROS stress can have beneficial effects, lead to stress fitness, and lifespan expansion of eukaryotic cells [Ristow et al., 2009; Zuin et al., 2010].

As to the sensitivity to SCO-1 of GBM TICs grown in different conditions, our results firstly showed that no major differences in cell viability after SCO-1 and SCO-1 plus NAC treatment were observed between cells grown on laminin or on matrigel. A second aspect to point is that differences in the IC50 determined at 48 h for GBM TICs grown in proliferating conditions with respect to that determined for cells obtained from GBM TICs grown in differentiating conditions are likely to be ascribed to a sink/buffering effect of the FBS present in the differentiation media (data not shown). In other words, the sensitivity of cultures enriched in GBM TICs to SCO-1 appeared similar to that displayed by cultures enriched in differentiated cells derived from the same GBM TICs. The hypothesis that the FBS reduced the availability or the activity of SCO-1, most likely through the presence of thiol-containing proteins, was also proven by experiments performed with HeLa cells treated with SCO-1 in the presence or absence of FBS. At equal SCO-1 concentration, the viability of the cells was higher in the presence of FBS than in its absence (data not shown).

In conclusion, our results indicate that the foremost mechanism responsible for the SCO-1 pro-apoptotic effect on human cancer cells is the generation of ROS in mitochondria and that this effect may be counteracted by the administration of NAC or sodium pyruvate. We suggest that SCO-1 may have a potential therapeutic value in cancer treatment, which deserves further investigation in animal models with a caveat concerning the assessment of an appropriate dosage.

ACKNOWLEDGMENTS

We thank Beatrice Dozin PhD for her help in editing our manuscript. This work was supported by Regione Liguria (Accordo collaborazione scientifica tra Liguria e Piemonte, per l'anno 2008), Compagnia di San Paolo (project 2007.0266).

REFERENCES

Abdel-Massih RM, Fares R, Bazzi S, El-Chami N, Baydoun E. 2009. The apoptotic and anti-proliferative activity of Origanum majorana extracts on human leukemic cell line. Leuk Res 34:1052–1056.

Akman SA, Forrest G, Chu FF, Esworthy RS, Doroshow JH. 1990. Antioxidant and xenobiotic-metabolizing enzyme gene expression in doxorubicin-resistant MCF-7 breast cancer cells. Cancer Res 50:1397–1402.

Alisi A, Balsano C. 2007. Enhancing the efficacy of hepatocellular carcinoma chemotherapeutics with natural anticancer agents. Nutr Rev 65:550–553.

Amme S, Rutten T, Melzer M, Sonsmann G, Vissers JP, Schlesier B, Mock HP. 2005. A proteome approach defines protective functions of tobacco leaf trichomes. Proteomics 5:2508–2518.

Arlorio M, Bottini C, Travaglia F, Locatelli M, Bordiga M, Coisson JD, Martelli A, Tessitore L. 2009. Protective activity of Theobroma cacao L. phenolic extract on AML12 and MLP29 liver cells by preventing apoptosis and inducing autophagy. J Agric Food Chem 57:10612–10618.

Bisio A, Romussi G, Russo E, Cafaggi S, Schito AM, Repetto B, De Tommasi N. 2008. Antimicrobial activity of the ornamental species *Salvia corrugata*, a potential new crop for extractive purposes. J Agric Food Chem 56:10468–10472.

Cataldi A. 2010. Cell responses to oxidative stressors. Curr Pharm Des 16:1387–1395.

Chan ED, Riches DW, White CW. 2001. Redox paradox: Effect of *N*-acetylcysteine and serum on oxidation reduction-sensitive mitogen-activated protein kinase signaling pathways. Am J Respir Cell Mol Biol 24:627–632.

Choi BK, Choi CH, Oh HL, Kim YK. 2004. Role of ERK activation in cisplatin-induced apoptosis in A172 human glioma cells. Neurotoxicology 25:915–924.

Chung WG, Miranda CL, Stevens JF, Maier CS. 2009. Hop proanthocyanidins induce apoptosis, protein carbonylation, and cytoskeleton disorganization in human colorectal adenocarcinoma cells via reactive oxygen species. Food Chem Toxicol 47:827–836.

Doroshow JH, Akman S, Chu FF, Esworthy S. 1990. Role of the glutathione-glutathione peroxidase cycle in the cytotoxicity of the anticancer quinones. Pharmacol Ther 47:359–370.

Fueyo J, Gomez-Manzano C, Liu TJ, Yung WK. 2001. Delivery of cell cycle genes to block astrocytoma growth. J Neurooncol 51:277–287.

Gangemi RM, Griffero F, Marubbi D, Perera M, Capra MC, Malatesta P, Ravetti GL, Zona GL, Daga A, Corte G. 2009. SOX2 silencing in glioblastoma tumor-initiating cells causes stop of proliferation and loss of tumorigenicity. Stem Cells 27:40–48.

Giannoni P, Narcisi R, De Totero D, Romussi G, Quarto R, Bisio A. 2010. The administration of demethyl fruticulin A from *Salvia corrugata* to mammalian cells lines induces ''anoikis'', a special form of apoptosis. Phytomedicine 17:449–456.

Ho E, Clarke JD, Dashwood RH. 2009a. Dietary sulforaphane, a histone deacetylase inhibitor for cancer prevention. J Nutr 139:2393–2396.

Ho YT, Lu CC, Yang JS, Chiang JH, Li TC, Ip SW, Hsia TC, Liao CL, Lin JG, Wood WG, Chung JG. 2009b. Berberine induced apoptosis via promoting the expression of caspase-8, -9, and -3, apoptosis-inducing factor and endonuclease G in SCC-4 human tongue squamous carcinoma cancer cells. Anticancer Res 29:4063–4070.

Hosack DA, De4nnis G, Jr., Sherman BT, Lane HC, Lempicki RA. 2003. Identifying biological themes within lists of genes with EASE. Genome Biol 4:R70.

Irizarry RA, Hobbs B, Collin F, Beazer-Barclay YD, Antonellis KJ, Scherf U, Speed TP. 2003. Exploration, normalization, and summaries of high density oligonucleotide array probe level data. Biostatistics 4:249–264.

Jazirehi AR, Bonavida B. 2004. Resveratrol modifies the expression of apoptotic regulatory proteins and sensitizes non-Hodgkin's lymphoma and multiple myeloma cell lines to paclitaxel-induced apoptosis. Mol Cancer Ther 3:71–84.

Kang MK, Kang NJ, Jang YJ, Lee KW, Lee HJ. 2009. Gallic acid induces neuronal cell death through activation of c-Jun *N*-terminal kinase and downregulation of Bcl-2. Ann NY Acad Sci 1171:514–520.

Karawajew L, Rhein P, Czerwony G, Ludwig WD. 2005. Stress-induced activation of the p53 tumor suppressor in leukemia cells and normal

lymphocytes requires mitochondrial activity and reactive oxygen species. Blood 105:4767–4775.

Kaur M, Velmurugan B, Tyagi A, Deep G, Katiyar S, Agarwal C, Agarwal R. 2009. Silibinin suppresses growth and induces apoptotic death of human colorectal carcinoma LoVo cells in culture and tumor xenograft. Mol Cancer Ther 8:2366–2374.

Koster AS. 1991. Bioreductive activation of quinones: A mixed blessing. Pharm Weekbl Sci 13:123–126.

Krzywanski DM, Dickinson DA, Iles KE, Wigley AF, Franklin CC, Liu RM, Kavanagh TJ, Forman HJ. 2004. Variable regulation of glutamate cysteine ligase subunit proteins affects glutathione biosynthesis in response to oxidative stress. Arch Biochem Biophys 423:116–125.

Lee J, Kotliarova S, Kotliarov Y, Li A, Su Q, Donin NM, Pastorino S, Purow BW, Christopher N, Zhang W, Park JK, Fine HA. 2006. Tumor stem cells derived from glioblastomas cultured in bFGF and EGF more closely mirror the phenotype and genotype of primary tumors than do serum-cultured cell lines. Cancer Cell 9:391–403.

Liu Y, Schubert DR. 2009. The specificity of neuroprotection by antioxidants. J Biomed Sci 16:98.

Monticone M, Biollo E, Fabiano A, Fabbi M, Daga A, Romeo F, Maffei M, Melotti A, Giaretti W, Corte G, Castagnola P. 2009. z-Leucinyl-leucinyl-norleucinal induces apoptosis of human glioblastoma tumor-initiating cells by proteasome inhibition and mitotic arrest response. Mol Cancer Res 7:1822–1834.

Nair S, Li W, Kong AN. 2007. Natural dietary anti-cancer chemopreventive compounds: Redox-mediated differential signaling mechanisms in cytoprotection of normal cells versus cytotoxicity in tumor cells. Acta Pharmacol Sin 28:459–472.

O'Brien PJ. 1991. Molecular mechanisms of quinone cytotoxicity. Chem Biol Interact 80:1–41.

Otto FJ. 1994. High-resolution analysis of nuclear DNA employing the fluorochrome DAPI. Methods Cell Biol 41:211–217.

Park C, Choi YW, Hyun SK, Kwon HJ, Hwang HJ, Kim GY, Choi BT, Kim BW, Choi IW, Moon SK, Kim WJ, Choi YH. 2009. Induction of G1 arrest and apoptosis by schisandrin C isolated from Schizandra chinensis Baill in human leukemia U937 cells. Int J Mol Med 24:495–502.

Pollard SM, Yoshikawa K, Clarke ID, Danovi D, Stricker S, Russell R, Bayani J, Head R, Lee M, Bernstein M, Squire JA, Smith A, Dirks P. 2009. Glioma stem cell lines expanded in adherent culture have tumor-specific phenotypes and are suitable for chemical and genetic screens. Cell Stem Cell 4:568–580.

Ristow M, Zarse K, Oberbach A, Kloting N, Birringer M, Kiehntopf M, Stumvoll M, Kahn CR, Bluher M. 2009. Antioxidants prevent health-promoting effects of physical exercise in humans. Proc Natl Acad Sci USA 106:8665–8670.

Robinson KM, Janes MS, Pehar M, Monette JS, Ross MF, Hagen TM, Murphy MP, Beckman JS. 2006. Selective fluorescent imaging of superoxide in vivo using ethidium-based probes. Proc Natl Acad Sci USA 103:15038–15043.

Rodriguez-Hahn L, Sanchez EBC, Cardenas J, Estebanes L, Soriano-Garcia M, Toscano R, Ramamoorthy TP. 1986. New highly oxidized diterpene quinones from Salvia fruticulosa (Labiatae). Tetrahedron Lett 27:5459–5462.

Saeed AI, Sharov V, White J, Li J, Liang W, Bhagabati N, Braisted J, Klapa M, Currier T, Thiagarajan M, Sturn A, Snuffin M, Rezantsev A, Popov D, Ryltsov A, Kostukovich E, Borisovsky I, Liu Z, Vinsavich A, Trush V, Quackenbush J. 2003. TM4: A free, open-source system for microarray data management and analysis. Biotechniques 34:374–378.

Sarkar FH, Li Y. 2004. Indole-3-carbinol and prostate cancer. J Nutr 134:3493S–3498S.

Seeram NP, Adams LS, Henning SM, Niu Y, Zhang Y, Nair MG, Heber D. 2005. In vitro antiproliferative, apoptotic and antioxidant activities of punicalagin, ellagic acid and a total pomegranate tannin extract are enhanced in combination with other polyphenols as found in pomegranate juice. J Nutr Biochem 16:360–367.

Slocombe SP, Schauvinhold I, McQuinn RP, Besser K, Welsby NA, Harper A, Aziz N, Li Y, Larson TR, Giovannoni J, Dixon RA, Broun P. 2008. Transcriptomic and reverse genetic analyses of branched-chain fatty acid and acyl sugar production in Solanum pennellii and Nicotiana benthamiana. Plant Physiol 148:1830–1846.

Woolard K, Fine HA. 2009. Glioma stem cells: Better flat than round. Cell Stem Cell 4:466–467.

Zuin A, Castellano-Esteve D, Ayte J, Hidalgo E. 2010. Living on the edge: Stress and activation of stress responses promote lifespan extension. Aging (Albany NY) 2:231–237.